Experiments on Control of a Soft Continuum Manipulator Robot

Clara Mayumi Bertolino Hamada
clara.hamada@usp.br
Instituto Superior Técnico, Universidade de Lisboa, Lisboa, Portugal

July 2021

Abstract

Continuum soft robots exhibit characteristics, such as compliance and dexterity, that offer greater security in human-robot interaction when compared to traditional robots. As a relatively recent field, continuum robotics has a potential growth not only in control but also in design. This study presents the construction, testing and control of a continuum soft robot to be used in the I-SUPPORT system, replacing the McKibben-based actuators used with silicone ones. After it was detailed the prototype's manufacturing, the mechanical and kinematics characterization were made comparing both actuators. The mechanical characterization was done by measuring the elongation of the single actuators by supplying pressure inputs. The kinematics characterization was made with the actuators assembled in the robot, including elongation, bending, reachable workspace and repeatability. The silicone actuators showed to be a good alternative, offering more reliability and easy maintenance to the manipulator. It was also proposed a control concept capable of solving the inverse kinematics using polynomial regression, which requires no prior knowledge about the robot. The effectiveness of the control was demonstrated by simulation data and experimentally, by an open-loop task space control using straight line, circle, and 8-shaped point-to-point trajectories. The results presented a promising control for the continuum soft robot proposed.

Keywords: Continuum robotics; Machine learning; Robot control; Polynomial regression; Soft actuators.

1. Introduction

The robots can be divided in three classifications based on links and joints [1]. The discrete robots are constructed by a series of rigid links connected by discrete joints, which corresponds to the traditional robots mechanism. The serpentine robots also have several discrete joints but they are connect by short rigid links, which results in smoother movements when compared to the discrete robots. The continuum robots do not contain any rigid links and joints, which increases their flexibility and dexterity in relation to the other two types of robot and produces curves in space even smoother than the serpentine robots.

Continuum robots are considered a new wave of robotics technology, they are inspired on biological structures, such as octopus tentacles, caterpillars, elephant trunks and worm bodies. These robots can be categorized in terms of their structural design, materials and actuation strategy [2].

In terms of mechanical structure the continuum robots are divided with respect of their segments and the presence of discs in their structure, which aim to enhance their functionalities. They are classified in four categories: single segment [3], multi-segment [4], single segment multi-disc [5] or multi-segment multi-disc [6].

There is a wide range of materials used for the design and assembly of the continuum robots. The bioinspiration of this type of robot is not limited to its shape, but also extends to the choice of materials they are made from, usually soft materials. Soft materials offer numerous advantages at potentially lower cost, such as lower impact force, which makes human-robot interaction safer; high flexibility and deformability, allowing adaptability to complex environments and energy absorption to maintain stability [7].

The range of actuators used in continuum robots is also wide, however, two of them are most common to be used: pneumatic actuators and tendon actuators [2]. According to the method and location of the mechanical actuation the continuum robots could be classified as intrinsic, extrinsic and hybrid [1]. In an intrinsic robot [6] the actuators are within the moving manipulator structure itself. In the extrinsic devices [8] the actuators are outside of the main structure, and work with a mechanical transmission of the forces. In the hybrid manipulators the actuation is based on a combination of

intrinsic and extrinsic actuation [3, 9].

As a relatively recent field in robotics, continuum robots' study has a potential growth not only in design but also in control [10]. The challenges involve modelling and controlling the robot's movements with positional accuracy, since analytical or numerical methods are very complex to be developed due to their virtually infinite DoF (Degrees-of-Freedom) motions and the restriction of using high-frequency controllers imposed by the nonlinear characteristics of the materials. The choice of the controller approach depends on the robot's application, design, actuator and sensor availability.

Model-based controllers rely on developing analytical models, they are the currently most widely used and studied strategy of control of the soft continuum robots [11]. The simplest modelling method is the Constant Curvature (CC) [12], which models the complex motion of the continuum robots, approximating it by a series of simple coupled motions. More complex models [13, 14] were developed, but although more accurate, these models computational and sensing cost increased dramatically, which ended up limiting their usage. After modelling the inverse kinematics (IK) problem should be solved by differential IK through the computation of the Jacobian [12], direct inversion [15] or as an optimization problem [16]. With the IK problem solved it could be applied different control strategies from open-loop [17] to closed-loop [14, 16].

Model-free controllers use machine learning techniques and empirical methods, such as neural networks [17, 18], multiagent reinforcement learning [5, 9]. These approaches are data dependent, which means that in order to obtain the trained models, real world data of the continuum robot should be acquired first. They have the advantage of being independent of the manipulator shape, but require high quality and large amount of data for training the models [11].

2. Reasearch Goals

This thesis was inspired by the I-SUPPORT service robotics system developed in the framework of the EU Horizon2020 Program applying soft robotics, adressing some of the challenges regarding its design, described in Section 3.2. It also adresses one of the most difficult tasks when using soft robot, control their motion, proposing a controller method that requires no prior knowledge about the actuators or the robot.The goals of this thesis project could be summarized in: (1) use of silicone actuators in the I-SUPPORT manipulator (Section 4), offering a fast and easy maintenance and making them less susceptible to manufacturing errors; (2) the kinematic characterization (Section 5.1) of the actuators assembled in the robot, which includes elongation, bending, reachable workspace and repeatability; (3) the mechanical characterization (Section 5.1) of the single actuators measuring the elongation of them under different pressures inputs; (4) open-loop controller method (Section 3.1) based on Holsten et. al [19], which uses polynomial regression to obtain the direct kinematic model of the robot; (5) tracking tests (Section 5.1) with straight line, circle and 8-shaped point-to-point trajectories to verify the controller proposed.

3. Materials and Methods

3.1. Control Method

To control the soft robot presented in this project a method based on the data driven approach proposed by Holsten et al. in [19] was applied. The method consists in five steps. It starts with data acquisition, sampled to cover the robot's workspace, collecting the vector parameters in a way with the corresponding actuator inputs. The sensor used should be able to acquire the robot's position (x, y, z) in P points, called here as shape vector, given to known actuators' input parameters. Hence, for the k^{th} robot's configuration it will be extracted a shape vector s given by Equation (1) corresponding to the inputs α given by Equation (2) of the N actuators.

$$s^k \equiv \begin{bmatrix} x_0^k & y_0^k & z_0^k & \dots & x_{P-1}^k & y_{P-1}^k & z_{P-1}^k \end{bmatrix}^T \quad (1)$$

$$\alpha^k \equiv \begin{bmatrix} \alpha_0^k & \alpha_1^k & \cdots & \alpha_{N-1}^k \end{bmatrix}^T \quad (2)$$

To create sub-domains of the workspace, the actuators inputs acquired were clustered using kmeans method. The labels obtained were used to divide also the shape vector parameters. This step allows to create local low-ordered models instead of a global higher order model, reducing the time complexity, the amount of data needed and increasing the accuracy of the models obtained. After the data partition, the models were built. The DK model is built assuming that the workspace could be described by a system of linear equations given by Equation (3), where S is the matrix of the shape vectors s for the k configurations, B is the matrix of the b vectors containing all the monomials up to degree equal to the order of the polynomial approximation and W is the weight coefficients matrix.

$$S = WB \quad (3)$$

where:

$$S \equiv \begin{bmatrix} s^0 & s^1 & \cdots & s^{k-1} \end{bmatrix} \quad (4)$$

$$B \equiv \begin{bmatrix} b\left(\alpha^0\right) & b\left(\alpha^1\right) & \cdots & b\left(\alpha^{k-1}\right) \end{bmatrix} \quad (5)$$

Each $b\left(\alpha^k\right)$ of the Equation (5) is obtained using the multinomial theorem. That make it possible to rewrite $b\left(\alpha^k\right)$ as a vector given by Equation (6),

where N is the number of actuators inputs α, the regression polynomial of order d and d_n all the possible numbers of non-negative integers adding up to the polynomial order approximation d.

$$b\left(\alpha^k\right) = \begin{bmatrix} 1 & M^1_{\alpha^k} & M^2_{\alpha^k} & \cdots & M^d_{\alpha^k} \end{bmatrix}^T \tag{6}$$

where

$$\begin{aligned} M^d_{\alpha^k} &= (\alpha_0 + \alpha_1 + \cdots + \alpha_{N-1})^d = \\ &= \sum_{d_0+d_1+\cdots+d_{N-1}=d} \prod_{n=0}^{N-1} \frac{\alpha_n^{d_n}}{d_n!} \end{aligned} \tag{7}$$

Using the data acquired, it is solved the linear system given by Equation (3), obtaining the weight matrix W that minimizes the value of the norm $\|(S - WB)\|$ and gives the relationship between the actuators inputs and the shape vectors. Hence, knowing the weight matrix W and given the actuators inputs α, the shape vector $s^*(\alpha)$ can be easily estimated using the Equation (8), that represents the DK model of the robot.

$$s^*(\alpha) = W b(\alpha) \tag{8}$$

Since it is an approximation and to guarantee security the function was clamped by the maximum and the minimum values of the cluster data used for training. The IK problem was solved finding the estimated actuators inputs α^* that minimizes the Euclidean distance between the desired position s_d and the one estimated using the DK model $s^*(\alpha^*)$.

$$\alpha^* \equiv \arg\min \|s_d - s^*(\alpha^*)\|^2 \tag{9}$$

Observing b given by Equation (6), since the first element is always 1, it is possible to rewrite it as Equation (10). Considering ω as the zeroth ordered weights, the weight matrix W could also be rewritten as Equation (11).

$$b = \begin{bmatrix} 1 \\ \hat{b} \end{bmatrix} \tag{10}$$

$$W = \begin{bmatrix} \omega & \hat{W} \end{bmatrix} \tag{11}$$

Then, we could rewrite Equation (8) as Equation (12), and substitute it in Equation (9), resulting in Equation (13) where just the second term depend on the estimated actuators inputs α^*.

$$\begin{aligned} s^* &= \begin{bmatrix} \omega & \hat{W} \end{bmatrix} \begin{bmatrix} 1 \\ \hat{b} \end{bmatrix} \\ s^* &= \omega + \hat{W}\hat{b} \end{aligned} \tag{12}$$

$$\alpha^* \equiv \arg\min \left\| (s_d - \omega) - \left(\hat{W}\hat{b}(\alpha^*)\right) \right\|^2 \tag{13}$$

For first order approximations, according to Equation (7), $\hat{b}$ corresponds simply to the actuators estimated inputs, therefore Equation (13) becomes a linear least square problem that could be solved through the Moore-Penrose pseudoinverse of $\hat{W}$ ($\hat{W}^+$) given by Equation (14). Again, the function was clamped by the minimum and maximum values of the actuators inputs inside the cluster.

$$\alpha^* = \hat{W}^+ (s_d - \omega) \tag{14}$$

For higher order approximations, the Equation (13) is nonlinear and an optimization method is convenient to be used. It was used a sequential quadratic programming to solve it, giving as initial conditions the model from Equation (14).

With the clustered data, a classification tree was trained. The pre-trained classification tree was used to predict the optimal local model to be used to obtain the predicted actuators input. In [19] is adopted two methods, a tree classifier and a minimum solution, and compared both of them. In this project it was opted to use the first one, because, based on the results obtained by Holsten et. al, it is a faster method. However, it could be less accurate due to the possibility of misclassifications.

To ensure that the method works properly, the B matrix in the linear system of the Equation (3) must be a full rank matrix. This condition makes it possible to obtain the weight matrix W. In order to have a full rank matrix, the number of linearly independent columns of B must be greater than or equal to the number of its rows. Therefore the minimum number of acquired data k_{min} is given by Equation (15).

$$k_{min} \geq \left[\sum_{i=1}^{d} \binom{N+i-1}{i} \right] + 1 \tag{15}$$

In polynomial regression, increasing the variability of the data makes it necessary to use polynomials of higher orders to approximate them. So, if the shape configurations have great variability, to describe the workspace of the robot it is necessary to use more complex polynomials. According to Equation (15), increasing d means to increase a lot the number of samples that must be acquired. Since collecting data is time consuming, the clustering step reduces the variability of the data, allowing to have lower order polynomials describing it. This approach is possible if every cluster have at least the minimum number of observations given by Equation (15). It was established that, if after 30 times trying to find a configuration that allows every cluster to have the minimum number of samples, the algorithm reveals that it is not possible to divide the data in the clusters with that specific polynomial order.

3.2. I-SUPPORT

The I-SUPPORT service robotics system envisions to support and enhance senior people to bathing, one of the activities classified as basic in the daily

living of people and that can offer difficult tasks for elderly, such as reaching their back and lower limbs to wash [20]. It is composed by a motorized chair and two soft robotic arms: one for provide pouring water and the other for scrubbing. The robotic arms are made of three interconnected modules. Although the modules have the same design, the proximal one is only actuated by cables and the middle and distal ones are identical and based on hybrid actuation, combining cables and pneumatic actuators. The hybrid actuation increases the overall functionality of the complete module, because it allows the actuators to complement each other regarding their limitations.

The most recently developed module prototype [5] is composed of three pneumatic actuators and three cables alternatively displaced at an angle of 60° in a circle of 60mm diameter. The 140mm diameter central channel in the circle is responsible for providing water and/or soap. All the actuators are decoupled, meaning that the cables have dedicated lines for tension regulation as the pneumatic actuators have for pressure. The total length of the module is 150mm and the total weight is 120g.

The pneumatic actuators used by [5, 9] are McKibben-based. The braid has a bellow-shaped surface, increasing the elongation performances, and the inner tube is a balloon made of latex silicone rubber. To guide the bending and, consequently, the application force of the soft robotic arm during its motion, in [5] a layer-by-layer reinforcement structure has been inserted along the module, in which the layers are distanced by 10mm from each other.

The module built by [9] accomplished satisfactorily the reachability necessary to the user workspace, covering larger distances with a reduced number of modules, and showed a stiffness variation, guaranteed by the hybrid actuation, to compensate internal/external loading in the bathing environment. However, since the actuator is manufactured in a bellow shape using manual mechanical deformation, it may result in an asymmetric shape not easily identified when the module is at rest. The friction between the internal chamber and the external braid during the actuator function may cause easily the rupture of the latex balloon, the replacement of it imply in the entire construction of a new actuator again, representing a time consuming maintenance. This lack of manufacturing precision together with the rapid degradation of the internal latex chamber of the actuators reduces their reliability, since each maintenance requires a new identification of the system, which means training the models all over again.

The McKibben-based I-SUPPORT was used to generate data for the Experimental (Section 5.1) phases of this project. For the Experimental tests, the data was acquired using one module of the I-SUPPORT. Its inputs are digit numbers from 0 to 255 that corresponds to a given pressure for the pneumatic actuators [21] and as output the end-effector position in the sensor reference frame.

3.3. Experimental Setup

The experiments described in Section 5.1 were developed using a pneumatic set that consists in three main parts inside an acrylic box: the pneumatic actuators (valves and filter regulators), the power supply (compressor) and the control unit (Arduino Due) [21].

It was used two sensors to capture the end-effector position of the robot. The SMART-DX motion tracking system [22] is a passive optical motion capture. The setup consists of six cameras placed around the support frame structure where the robot was uphold with three markers attached to its tip. The data is acquired with a high frequency rate, in which each input results in a step response of the system. Thus the data was pre-processed using a Gaussian-weighted moving average filter to obtain steady state to perform the analysis. The final position of the tip was taken from the average of the x, y and z positions of the markers.

The Aurora System [23] is an advanced electromagnetic spatial measurement system that calculates the position and the orientation of a six DoF embedded sensor within a defined volume. The sensor was attached at the end of the manipulator. It was created a MATLAB script to acquire the robot's position and orientation after some seconds after the given input, so the outputs were the positions of the robot already in the steady state.

4. Prototype Description

The proposed robotic arm follow the same structure of the module prototype of the I-SUPPORT developed in [5] and described in Section 3.2, being composed of three distinct parts: the base, the guiding structure and the actuators. A rigid rectangular base made of Plexiglas is used to place the robot in the support frame structure, allowing its movements, and to uphold the pneumatic connectors and the cable set-up. A central hole of 10mm was inserted to facilitate the flow of water and soap, but it will also be used as a mechanical connection between the manipulator and its base.

There are two types of discs in the robot manipulator. On the proximal and distal extremities of the pneumatic actuators, a Plexiglas disc of 5mm thickness is attached. In the proximal, the central hole, besides of working as a water and soap channel, will hold the mechanical connection with the base. Therefore, these discs act mainly as connectors between the parts of the prototype. Additionally,

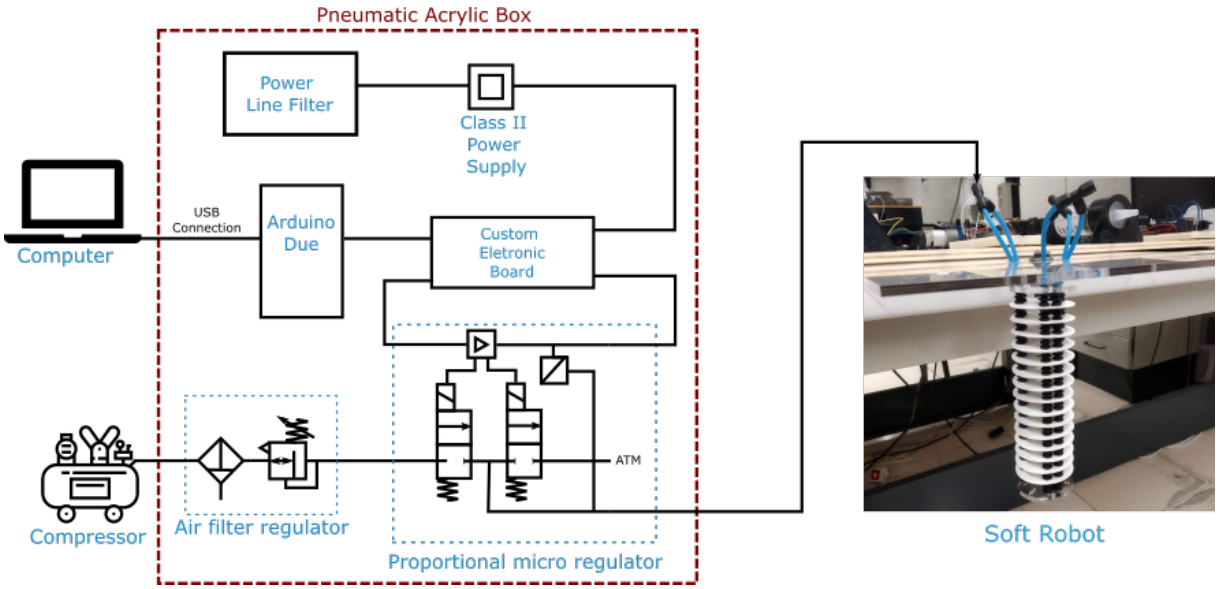

Figure 1: Final Assembly

fifteen central discs of 1.2mm thickness polypropylene were placed equally spaced between the actuators act as a reinforcement structure. They are responsible to lead the application of the force of the manipulator through the guiding of the bending during its motion.

The main difference of the proposed robot rely on the pneumatic actuators. This work proposes the use of silicone bellows as actuation system, trying to increase the reliability and facilitate the maintenance of the robot. In the retail market, the only silicone bellows found available with 10mm of external diameter and uniform shape was 10cm length. In order to mantain the dimensions of the I-SUPPORT, to build an actuator it was joined two units of the bellows using silicone glue. Besides the fast cure and durability, the silicone glue makes the connection uniform and smooth. It can also be used for repair of the silicone actuators, which makes the maintenance really easy.

The connection, before made only with the Y connectors and pneumatic tubes, will be made using a threaded tube, locked with washers and nuts, where the tooth washer prevent the nuts from backing out and the flat washer distribute the load in the base and the disc. The mechanical connection offers more reliability since the robot's weight will be hold by it and not by the linkage between the tubes inside the Y connectors.

The actuators are inserted in the holes designed in the polypropylene discs, letting them equally spaced. The extremities of the chambers are inserted in the acrylic discs. The distal extremity's holes are closed and in the proximal extremity's ones the pneumatic tubes are inserted and connected to the Y connectors.

The acrylic pneumatic box described in Section 3.3 has four outside connections. The power supply plug is connected into an outlet. To each of the three proportional micro regulators a pneumatic tube is attached. The other extremity of the tube is coupled to a pair of silicone actuator by the Y connectors. The USB connection communicates with the computer, which will make it possible to control the manipulator. The compressor is connected to the air filter regulator by a pneumatic tube, and also is plugged into an outlet. The final assembly described can be seen in Figure 1, for simplicity, it is only showed one proportional micro regulator connected to a pair of actuators, the other two are equally connected to the filter, the custom board and a pair of actuators.

5. Results

5.1. Experimental

Single Actuators Pressure vs Elongation

This test goal was to chracterize the behaviour of the silicone actuator and the McKibben-based one, without load. To simulate the constrains imposed by the discs, it was placed mechanical washers equally spaced along the actuators. The elongation was measured with a measuring tape that was fixed on a bench. Initially, both the actuators were measured without any pneumatic input, the second input was only registered when the actuators presented some visual elongation movement and from there on the pressure was gradually increased. The ultimate input was registered when no further elongation was observed in the actuators and the surface showed some evidences that the volume capacity was almost at its limits.

In Figure 2 it is possible to see the results of

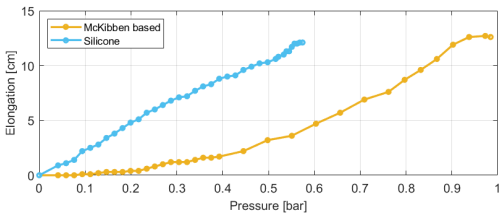

Figure 2: Elongation per pressure of the McKibben-based and the silicone actuators

the experiment, since the initial length of the actuators differ in 1.6cm, the plot was made with respect to the initial length. The McKibben-based actuator showed at the limit a slightly higher elongation, 0.5cm bigger than the Silicone one. The Silicone actuator presented a linear behaviour from the beginning to the end of the test. On the other hand, the McKibben-based actuator presented a parabolic behaviour, probably due to the mechanical resistance imposed by the braid of the McKibben-based actuator which allows a higher stiffness compared to the silicone actuator.

Kinematic Characterization

In the experimental tests characterizing the manipulator's functionalities with the silicone actuators, a comparison will be made between the proposed robot and the one that uses the McKibben-based actuator. Based on the maximum elongation of the single actuators obtained and the behaviour of the actuators assembled in the robot, it was selected the maximum pressures or, essentially the valve set-point reference value coded as an 8 bit integer, that would be work with during the following experiments. All the results will be showed with respect to the starting configuration. The data acquired were all static, but the time it takes for the robots to reach the steady state position is different: the McKibben-based actuators robot takes 2s against 5s of the silicone actuators robot.

- **Elongation**

The elongation corresponds to the activation of all the three chambers at the same time with the same pressure. It was used three values of pressure: 0, 0.06bar and 0.48bar for the robot assembled with silicone actuators and 0, 0.16bar and 0.69bar for the robot assembled the McKibben-based one. The results showed the silicone robotic arm presenting a higher initial elongation of 1.012cm with respect to the initial position against just 0.5cm for the McKibben-based, the maximum elongation was higher in the latter. Considering the single actuators results (Section 5.1), the elongation of 9.615cm presented by the robot assembled with the McKibben-based actuators be slightly higher than the elongation of 9.197cm from the silicone robot was already expected. Although all the actuators were activated at the same time with the same input pressure, the robots did not follow a strictly straight line towards the ground. In fact, both robots presented a deviation from the origin.

- **Bending**

The bending will be evaluated in two different activation patterns, in which the robot will be subject to two conditions: with a tendon constrain and without it. First it was performed a test activating only one pneumatic chamber, suppling it with 11 pressure values, from 0 to 0.48bar for the silicone manipulator and from 0 to 0.69bar for the McKibben-based one.

Figures 3 and 4 illustrate the resulting behaviour of this activation pattern for both robots without the tendon constraint. The z-axis displacement of the McKibben-based manipulator is almost twice of the one showed by the robot with silicone actuators. It is also possible to notice that the McKibben-based manipulator showed a pure bending movement, from the initial position it can be seen that increasing the chamber pressure results in the robot always going up and right. The behaviour of the silicone robot when activating one chamber is characterized by a diagonal elongation movement followed by a smooth bending. The final orientation of tip during the bending movement is similar in both of them.

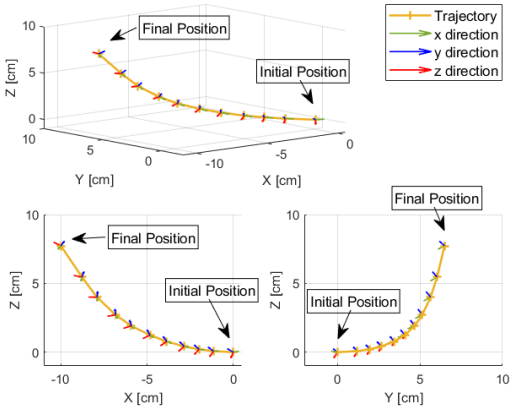

Figure 3: Global bending movement with the activation of one pneumatic chamber of the robot assembled with the McKibben-based actuators.

To add the tendon constrain in the robots, one of the holes made in the distal disc of reinforcement structure was chosen to host the tendon. The tendon was passed through all the consecutive and parallel discs of the structure until it reaches the base, where it was fixed ensuring that the robot's natural length was maintained. To carry out

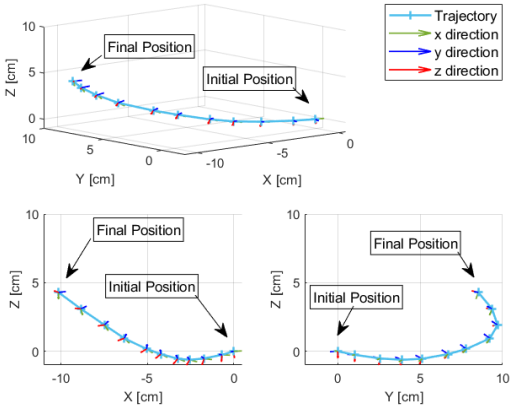

Figure 4: Global bending movement with the activation of one pneumatic chamber of the robot assembled with the silicone actuators.

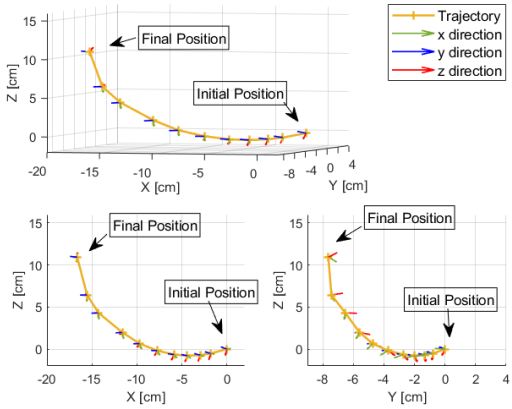

Figure 5: Global bending movement with the activation of two adjacent pneumatic chambers restrict by tendons of the robot assembled with the McKibben-based actuators.

the experiments, the activated pneumatic chamber was the one that was diametrically opposite. The resulting behaviour of this activation pattern for both robots when compared to the results obtained without the tendon contraints, was pratically the same. One may affirm that the tendon did not have influence in the global bending movement for both robots, since the overall final position and the shape of the trajectory are almost equal in both conditions.

The second activation pattern results from the activation of two adjacent pneumatic chambers, following the same procedure of the first one. For the experiment without tendoms, both robots presented an accentuated diagonal elongation first, followed by a bending, starting just in the last three input pressures for both robots. Diverging from the movement obtained with one chamber in which bending movement predominated. Due to this behaviour the final position of the end-effector is lower than the initial position, but with changed orientation. The z-direction displacement of the McKibben based robot is slightly higher than the silicone one, as well as the x and y-direction displacement. For the silicone arm, again, with the highest pressure inputs the robot starts to approximates to the initial position in the y-direction.

Figures 5 and 6 illustrate the resulting behaviour of the second activation pattern for both robots with the tendon constraint. Unlike the results obtained using one chamber, the added constrains evolved in a completely different behaviour of the manipulators when compared to the unrestricted movement. The McKibben-based manipulator (Figure 5) the bending reaches approximately 10cm in the z-direction, the highest position recorded in the tests carried out in this project. Like the previous tests, the increase of the pressure makes the robot's tip to move away from the initial position in

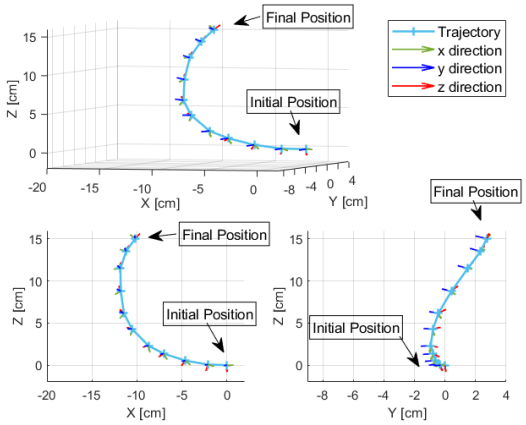

Figure 6: Global bending movement with the activation of two adjacent pneumatic chambers restrict by tendons of the robot assembled with the silicone actuators.

x and y directions. The silicone manipulator (Figure 6) reaches an even higher position than the McKibben-based constrained manipulator, 15cm from the initial position. It is possible to see that the silicone robot starts to bending over itself with the highest input pressures.

- **Reachable workspace**

The workspace test aims to measure all the reachable positions of the end-effector of the robot. In order to do that it was acquired a total of 8000 points, resulted from a permutation of the three pneumatic inputs using twenty values equally spaced between 0 and 0.48bar for the silicone robot and between 0 and 0.69bar for the McKibben-based one. The results of the experiments regarding the initial position can be seen in Figures 7 and 8.

The overall shape of the workspace for both robots can be categorized as a volumetric convex with the limits defined by the maximum bending and elongation capabilities, and the xy-view

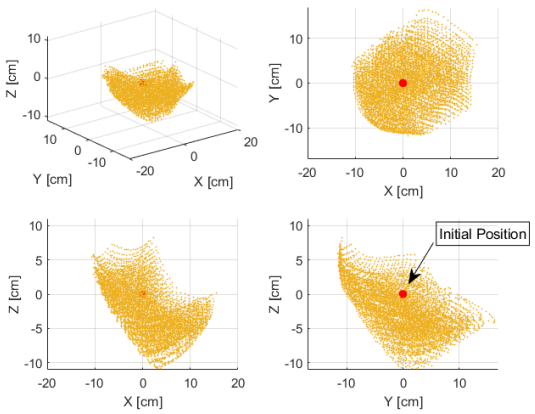

Figure 7: Workspace evaluation for the single module assembled with the McKibben-based actuators. The red point represents the initial position of the module in an unactivated state.

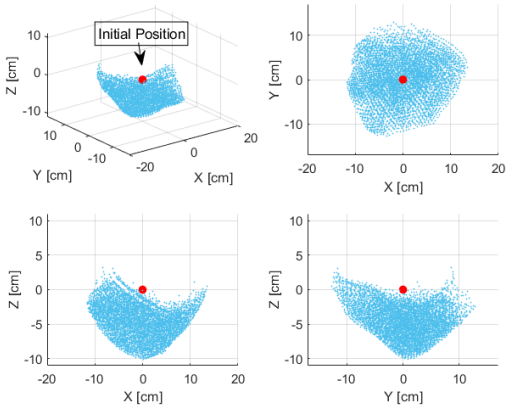

Figure 8: Workspace evaluation for the single module assembled with the silicone actuators. The red point represents the initial position of the module in an unactivated state.

showed a circular-like shape. The McKibben-based module presented a range of 26.0cm, 28.1cm and 19.1cm for the x, y and z directions respectively. A range slightly higher than the results presented by the silicone manipulator, 25.1cm, 25.5cm and 13.2cm for the x, y and z directions respectively. Although the McKibben-based manipulator showed a better reachability it is possible to see that the silicone module offers a symmetrical motion in every direction. The asymmetry of the shape in the McKibben-based module, as already identified by Ansari et al. in [9], can be attributed to the manufacturing procedure, in which the manual deformation of the braid could result in irregularities that end up being increased when the robot is assembled with the six actuators.

- **Repeatability**

The evaluation of the repeatability corresponds to a statistical characterization of the modules verifying how repeatable the positions of the workspace are. To perform this test it was chosen three random pneumatic inputs of each condition studied: bending due to one chamber, bending due to two chambers and elongation, that were reached from twenty different random input values from the set of data that resulted on the reachable workspace, starting at the rest position. It was performed 9 tests with different goal points, each one with 20 samples, which sum 180 points. For each test, the 20 samples of the chosen point acquired were normalized centering the data to have mean 0. The normalized data acquired is showed in the histogram of Figure 9, in which each bar width is 0.1cm.

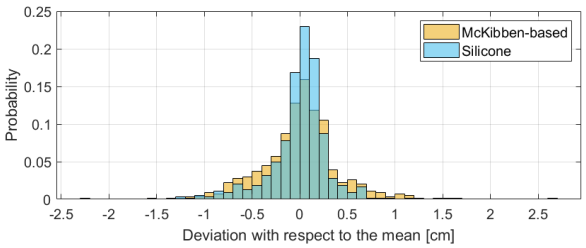

Figure 9: Histogram of the data acquired with nine different goal points that were normalized to zero mean for each manipulator assembled with the actuators.

Although both robots showed most samples around 0.5cm of deviation, the McKibben-based module presented as maximum deviation during the tests 2.7cm, while the silicone module presented 1.5cm, almost half of the value presented by the other manipulator. The silicone robot also exhibits 94% of the data within 0.61cm of deviation from the mean values, against 0.86cm showed by the McKibben-based robot. Regarding the repeatability the manipulator assembled with the silicone actuators demonstrates a better performance not only with respect to the maximum values but also to the value inside of the confidence interval that were both smaller.

Control

Using the acquired data describing the reachable workspace, it was performed an analysis under different conditions to define which models describe the kinematics of the robot better. The analysis revealed that for the DK model, after 14th order, the training error stops to reduce and begins to increase for higher orders, which indicates that the order of the model should not be higher than 14th. While, the errors of training and validation for the IK model decreasing until polynomials of 4th orders, not at 14th order as was expected.

After testing several combinations of polynomial order and the clusters, the lower error amongst the DK models obtained were given by 8 clusters of 6th

Table 1: Validation error for the DK and IK models using selected combinations of order and clusters for the silicone manipulator

		Model Errors	
Cluster	**Order**	**Direct Kinematic**	**Inverse Kinematic**
14	3	2.49 ± 0.61 mm	1444.65 ± 30.51 Pa
8	6	2.05 ± 0.60 mm	1986.52 ± 77.27 Pa
13	4	2.32 ± 0.50 mm	1510.04 ± 39.36 Pa

order and for the IK model it was reached using 14 clusters of 3rd order. It was also selected a combination of order and clusters that gives the lower mean square error between the DK and IK errors. The values obtained can be seen in Table 1.

The models of Table 1 were used to perform point-to-point trajectories in the space with the real manipulator. The positions in the space that described a chosen trajectories were given as inputs to the IK model. This allowed to obtain the pressure that would be supplied to the pneumatic actuators of the silicone manipulator and would result in the trajectories characterizing an open-loop controller. The distance between two consecutives points in the trajectories was set to approximately 4mm. This value was defined by test changing the distance and evaluating the trajectory error, considering that the error does not change significantly, a deep analysis was not carried out.

It was tested three different trajectories: a straight line, a circle and a 8-shaped trajectory. To enable the manipulator to perform the trajectories, they should be within the limits of the workspace of the robot, but an attempt was also made to occupy a considerable area with the curves, varying all their coordinates. The models of Table 1 were trained with five different sets of data randomly selected from the 8000 points, following the separation of training data previously set at 70%.

The mean error and the standard deviation of the point-to-point trajectories for all the data sets tested can be seen in Table 2, the marked cells represent the lowest error for each model in each trajectory. Observing the marked cells, it cannot be stated that one data set was better than the others as well as the models. Although the same data set, the second one, resulted in the best performance for all the trajectories, the models with which it was obtained were different.

Comparing the experimental results of Table 2 with the theoretical ones from Table 1, one may noticed that the experimental errors are around 4, 5 times bigger than the theoretical results of the DK model. It was already expected higher errors, since the pneumatic inputs for the robot are obtained from the IK model that has an associated error, these inputs are then sent to the robot which, in addition to its own natural frequency oscillation, presents external noise, such as the oscillations introduced the operation of the pneumatic set.

6. Conclusions

This thesis presents the construction, testing and control of a continuum soft robot to be used in the I-SUPPORT system. This work proposed the use of silicone actuators in the robotic arm of the system, aiming to offer more reliability and easy maintenance to the manipulator. By obtaining the kinematics models of the robot through polynomial regression method based on Holsten et al. [19], an open-loop controller is proposed that does not require prior knowledge about the robot.

The manufacturing of the proposed silicone actuators is easy, inexpensive and fast, it only needs the silicone bellows, scissors and the specific glue. In case it presents some small holes in the surface, it could be easily repaired using the glue to cover them. Due to this characteristics, a symmetrical shape for the robot is obtained without great effort. The symmetrical shape achieved in the manufacturing of the actuators, reflected in the reachable workspace and the repeatability of the robot. The experiments showed for the silicone robot a symmetrical motion in every direction, although slightly lower reachability than the manipulator assembled with the McKibben-based actuators. The silicone assembled also presented better results regarding the repeatability, offering more reliability, which makes it easier to modelling and control.

The silicone offers less stiffness when compared to the McKibben-based actuators. Studying the single actuators, it was observed that this characteristic offers a more linear relationship between pressure and elongation, but also implies in more time to reach the steady state condition for the silicone actuator. The silicone actuators have the ability to work with negative pressures, which could enhance the kinematic characteristics observed during the experiments, such as improving the bending capabilities and increasing the overall workspace. Due to availability, this ability has not been addressed, but could be explored in future work.

The model-free control was tested obtaining the IK and DK models for the robot for different sets of training data and combinations of polynomial order and clusters. In all the experiments the controller presented good results in describing the point-to-point trajectories proposed with mean errors varying from 8.5 to 12mm. These results could be improved implementing a closed-loop control. However, the experiments revealed the challenge of defining a unique combination of order and clusters that best describes the robot's kinematics, depending on the trajectory to be described, one combination stands out in relation to the others. The

Table 2: Mean error and standard deviation for all the data sets randomly selected, models obtained and trajectories tested.

		Point-to-point Trajectory Error [mm]		
Model	**Data Set**	**Straight Line**	**Circle**	**8-Trajectory**
8 cluster of 6th order	**1**	12.70 ± 5.11	9.34 ± 3.50	11.46 ± 2.37
	2	9.46 ± 2.92	8.43 ± 2.81	9.90 ± 3.71
	3	10.22 ± 3.19	8.94 ± 2.94	9.18 ± 2.85
	4	10.41 ± 2.33	8.91 ± 3.40	9.79 ± 5.88
	5	10.28 ± 2.15	8.86 ± 3.44	9.96 ± 3.43
14 cluster of 3rd order	**1**	10.52 ± 3.05	8.80 ± 3.74	10.21 ± 3.74
	2	9.04 ± 2.16	8.59 ± 3.06	9.28 ± 2.93
	3	10.50 ± 2.49	9.80 ± 3.86	9.88 ± 3.21
	4	10.39 ± 2.42	8.97 ± 3.24	9.15 ± 1.98
	5	10.45 ± 2.89	8.88 ± 3.30	9.07 ± 2.40
13 cluster of 4th order	**1**	10.19 ± 2.61	8.53 ± 3.65	10.35 ± 1.78
	2	11.00 ± 5.27	8.85 ± 3.05	8.67 ± 2.49
	3	9.43 ± 2.02	9.22 ± 3.30	10.51 ± 3.48
	4	9.89 ± 2.45	8.73 ± 3.47	9.39 ± 2.56
	5	9.96 ± 2.52	9.12 ± 3.36	9.15 ± 2.34

hope is that using this work, a more structured approach can be taken to analyze and tackle the control problems related to the proposed silicone actuators in the I-SUPPORT robotic arm.

References

[1] G. Robinson and J. B. Davies, "Continuum robots - a state of the art," in *Proceedings 1999 IEEE International Conference on Robotics and Automation (Cat. No.99CH36288C)*, vol. 4, pp. 2849–2854, 1999.

[2] S. Kolachalama and S. Lakshmanan, "Continuum robots for manipulation applications: A survey," *Journal of Robotics*, vol. 2020, 2020.

[3] B. A. Jones, M. William, and I. W. Clemson, "Design and Analysis of a Novel Pneumatic Manipulator," *IFAC Proceedings Volumes*, vol. 37, no. 14, pp. 687–692, 2004.

[4] W. McMahan, B. A. Jones, and I. D. Walker, "Design and implementation of a multi-section continuum robot: Air-Octor," in *2005 IEEE/RSJ International Conference on Intelligent Robots and Systems*, pp. 2578–2585, 2005.

[5] Y. Ansari, M. Manti, E. Falotico, M. Cianchetti, and C. Laschi, "Multiobjective Optimization for Stiffness and Position Control in a Soft Robot Arm Module," *IEEE Robotics and Automation Letters*, vol. 3, pp. 108–115, jan 2018.

[6] M. Rolf and J. J. Steil, "Constant curvature continuum kinematics as fast approximate model for the Bionic Handling Assistant," in *2012 IEEE/RSJ International Conference on Intelligent Robots and Systems*, pp. 3440–3446, 2012.

[7] S. Kim, C. Laschi, and B. Trimmer, "Soft robotics: A bioinspired evolution in robotics," *Trends in Biotechnology*, vol. 31, no. 5, pp. 287–294, 2013.

[8] M. Cianchetti, A. Arienti, M. Follador, B. Mazzolai, P. Dario, and C. Laschi, "Design concept and validation of a robotic arm inspired by the octopus," *Materials Science and Engineering: C*, vol. 31, no. 6, pp. 1230–1239, 2011.

[9] Y. Ansari, M. Manti, E. Falotico, Y. Mollard, M. Cianchetti, and C. Laschi, "Towards the development of a soft manipulator as an assistive robot for personal care of elderly people," *International Journal of Advanced Robotic Systems*, vol. 14, mar 2017.

[10] C. Laschi, B. Mazzolai, and M. Cianchetti, "Soft robotics: Technologies and systems pushing the boundaries of robot abilities," *Science Robotics*, vol. 1, no. 1, pp. 1–12, 2016.

[11] T. G. Thuruthel, *Machine Learning Approaches for Control of Soft Robots*. PhD thesis, Scuola Superiore Sant'Anna, 2018.

[12] M. W. Hannan and I. D. Walker, "Kinematics and the implementation of an elephant's trunk manipulator and other continuum style robots," *Journal of Robotic Systems*, vol. 20, no. 2, pp. 45–63, 2003.

[13] D. Trivedi, A. Lotfi, and C. D. Rahn, "Geometrically exact dynamic models for soft robotic manipulators," in *2007 IEEE/RSJ International Conference on Intelligent Robots and Systems*, pp. 1497–1502, 2007.

[14] I. A. Gravagne, C. D. Rahn, and I. D. Walker, "Large deflection dynamics and control for planar continuum robots," *IEEE/ASME Transactions on Mechatronics*, vol. 8, no. 2, pp. 299–307, 2003.

[15] D. B. Camarillo, C. R. Carlson, and J. K. Salisbury, "Configuration Tracking for Continuum Manipulators With Coupled Tendon Drive," *IEEE Transactions on Robotics*, vol. 25, no. 4, pp. 798–808, 2009.

[16] D. B. Camarillo, C. R. Carlson, and J. K. Salisbury, "Task-Space Control of Continuum Manipulators with Coupled Tendon Drive," in *Khatib O., Kumar V., Pappas G.J. (eds) Experimental Robotics. Springer Tracts in Advanced Robotics, vol 54. Springer, Berlin, Heidelberg.*, pp. 271–280, 2009.

[17] M. Giorelli, F. Renda, M. Calisti, A. Arienti, G. Ferri, and C. Laschi, "Neural Network and Jacobian Method for Solving the Inverse Statics of a Cable-Driven Soft Arm with Nonconstant Curvature," *IEEE Transactions on Robotics*, vol. 31, no. 4, pp. 823–834, 2015.

[18] T. G. Thuruthel, E. Falotico, M. Manti, A. Pratesi, M. Cianchetti, and C. Laschi, "Learning closed loop kinematic controllers for continuum manipulators in unstructured environments," *Soft Robotics*, vol. 4, pp. 285–296, sep 2017.

[19] F. Holsten, M. P. Engell-Norregard, S. Darkner, and K. Erleben, "Data driven inverse kinematics of soft robots using local models," *Proceedings - IEEE International Conference on Robotics and Automation*, vol. 2019-May, pp. 6251–6257, 2019.

[20] European Union's Horizon 2020, "I-support." (Accessed: 15.10.2019).

[21] The BioRobotics Institute - Sant'Anna School of Advances Studies, Viale Rinaldo Piaggio, 34 - 56025 Pontedera(PI), Italy, *Soft Manipulator - User Manual*.

[22] SMART-DX Motion Tracking Systems. (Accessed: 15.11.2020).

[23] Northern Digital Inc., Waterloo, Ontario, Canada N2V 1C5, *Aurora V2 User Guide - Revision 3*, July 2012.